NUCLEAR THEORY, Vol. 30 (2011)
eds. A. Georgieva, N. Minkov, Heron Press, Sofia

Full Solution of Nuclear Quadrupole-Octupole Model

M. Strecker[1], **N. Minkov**[1,2], **H. Lenske**[1]

[1]Institut für Theoretische Physik der Justus-Liebig-Universität, Heinrich-Buff-Ring 16, D–35392 Giessen, Germany

[2]Institute of Nuclear Research and Nuclear Energy, Bulgarian Academy of Sciences, Tzarigrad Road 72, BG-1784 Sofia, Bulgaria

Abstract. A collective model of nuclear quadrupole-octupole vibrations and rotations, originally restricted to a coherent interplay between quadrupole and octupole modes, is now developed for application beyond this restriction. The eigenvalue problem is solved by diagonalizing the unrestricted Hamiltonian in the basis of the analytic solution obtained in the case of the coherent-mode assumption. Within this scheme the yrast alternating parity band is constructed by the lowest eigenvalues having the appropriate parity at given angular momentum. This model scheme was applied to describe the alternating parity spectra of several rare-earth nuclei: ^{150}Nd, ^{152}Sm, ^{154}Gd and ^{156}Dy. It was obtained that the unrestricted model calculations (without coherent interplay) provide a better description with the root-mean square (RMS) deviation being smaller than the one in the analytic solution.

1 Introduction

The collective motion of atomic nuclei is mainly governed by the shape deformations and the interplay between different kinds of deformation degrees of freedom [1]. An important role is played by the quadrupole-octupole motion which provides a specific structure of the spectrum, with the presence of alternating-parity bands and split parity-doublet levels in even-even and odd-mass nuclei, respectively [2]. A specific indication for the presence of quadrupole-octupole collectivity is the observation of enhanced electric E1 and E3 transitions between levels with opposite parity. In even-even nuclei the negative-parity sequence is shifted up with respect to the positive parity sequence. This "parity shift" effect is explained as the result of a tunneling of the system between the two opposite orientations along the principal symmetry axis [3]- [5]. The magnitude of the energy shift corresponds to the softness of the shape with respect to the octupole deformation. Generally, one can classify the quadrupole-octupole spectra of even-even nuclei in two groups corresponding to the motion of stiff and soft reflection-asymmetric deformations. In the stiff regime of motion the negative and positive parity sequences merge at certain angular momentum into

a single rotation band called "octupole band". Such kind of spectra are typically observed in the light actinide nuclei Rn, Ra and Th. In the soft regime of quadrupole-octupole motion the opposite parity sequences remain well separated from each other along the whole angular momentum region. Typical examples of such kind of spectra are observed in the heavier actinides U and Pu and some rare-earth isotopes like Nd, Sm, Gd and Dy. Some model approaches were specially developed to describe the soft quadrupole-octupole motion [6]- [8].

Especially in [8] Minkov *et al.* have applied a coherent quadrupole-octupole motion (CQOM) model to the four nuclei ^{150}Nd, ^{152}Sm, ^{154}Gd and ^{156}Dy. This model is described in more detail in the next section. As a result of a fitting procedure applied to four model parameters for each nucleus, the yrast spectra of these rare-earth even-even nuclei could be described with an accuracy of about 50 keV for the root mean square deviation of theory and experiment.

This model has the advantage to be completely solvable in an analytic way. However, in order to reach this analytic solution certain correlations between the parameters of the initial Hamiltonian are imposed. These additional correlations, which have to hold, especially imply the same oscillation frequency for the quadrupole and the octupole degree of freedom ($\omega = \omega_2 = \omega_3$). As a consequence, the energy potential, which enters the Schrödinger equation, is limited to the case of having an ellipsoidal minimum with respect to the quadrupole and octupole deformation variables β_2 and β_3. Therefore the application of this model is restricted to a special class of solutions. On the other hand the unrestricted Hamiltonian allows the presence of more general shapes, providing the possibility to describe more general properties of the collective motion.

The purpose of the present work is to develop the model beyond the coherent case of equal oscillation frequencies, thereby allowing the model Hamiltonian to unfold its full capability. It follows that the underlying task is to obtain a full solution of the two-dimensional Schrödinger equation. This can only be done in a numerical way. In the present work the problem is solved by diagonalizing the Hamiltonian in the basis of the analytic wave functions obtained in the coherent case [8]. As a result one obtains an yrast spectrum which depends on model parameters. These are fitted to obtain the best agreement between theory and experiment. It will be seen below that the quality of the model description could be improved in comparison to the CQOM description for the considered nuclei. In addition, the developed approach allows one to give a clearer physical interpretation of the obtained model parameters, especially in relation to the shape of the model potential.

2 Two-Dimensional Quadrupole-Octupole Model

2.1 General Hamiltonian

The starting point is a vibration-rotation Hamiltonian formulated in the collective axial quadrupole and octupole deformation variables β_2 and β_3 [8]

$$H_{qo} = -\frac{\hbar^2}{2B_2}\frac{\partial^2}{\partial\beta_2^2} - \frac{\hbar^2}{2B_3}\frac{\partial^2}{\partial\beta_3^2} + \frac{1}{2}C_2\beta_2^2 + \frac{1}{2}C_3\beta_3^2 + \frac{X(I)}{d_2\beta_2^2 + d_3\beta_3^2}\,, \quad (1)$$

where $X(I) = \frac{1}{2}[d_0 + I(I+1)]$ for even-even nuclei. B_2 and B_3 are mass parameters, C_2 and C_3 are stiffness parameters, d_2 and d_3 are moment of inertia parameters and d_0 determines the potential core at angular momentum $I = 0$. The overall shape of the potential is governed by a quadratic growth for larger deformations and a strongly repulsive potential centre.

2.2 Coherent Solution

The transition to ellipsoidal coordinates given by

$$\eta = \left[\frac{2(d_2\beta_2^2 + d_3\beta_3^2)}{d_2 + d_3}\right]^{\frac{1}{2}} \quad \text{and} \quad \phi = \arctan\left(\frac{\beta_3}{\beta_2}\sqrt{\frac{d_3}{d_2}}\right) \quad (2)$$

and the imposition of the relations $B := \frac{d}{d_2}B_2 = \frac{d}{d_3}B_3$ and $C := \frac{d}{d_2}C_2 = \frac{d}{d_3}C_3$, where $d = (d_2 + d_3)/2$, allow one to obtain the energy spectrum in the following closed formula [8]

$$E_{n,k} = \hbar\omega\left[2n + 1 + \sqrt{k^2 + b\cdot X(I)}\right]\,, \quad (3)$$

where $\omega = \sqrt{C/B}$ and $b = 2B/\hbar^2 d$ are considered as fitting parameters. The model wavefunction has the form

$$\Psi^{\pi}_{nIM0}(\eta,\phi) = \sqrt{\frac{2I+1}{8\pi^2}}D^I_{M\,0}(\theta)\Phi^{\pi}_{nkI}(\eta,\phi)\,, \quad (4)$$

where $D^I_{M\,0}(\theta)$ is the Wigner rotation function and

$$\Phi^{\pi}_{nkI}(\eta,\phi) = \psi^I_{nk}(\eta)\varphi^{\pi}_k(\phi) \quad (5)$$

is the quadrupole-octupole vibration function. Here

$$\psi^I_{n,k}(\eta) = \sqrt{\frac{2c\Gamma(n+1)}{\Gamma(n+2s+1)}}e^{-c\eta^2/2}(c\eta^2)^s L_n^{2s}(c\eta^2) \quad (6)$$

is the "radial" part of $\Phi(\eta,\phi)$ with $c = \sqrt{BC}/\hbar$ and $s = (1/2)\sqrt{k^2 + bX(I)}$ as well as

$$\varphi^+_k(\phi) = \sqrt{2/\pi}\cos(k\phi)\,, \quad k = 1,3,5,\ldots \quad (7)$$

$$\varphi^-_k(\phi) = \sqrt{2/\pi}\sin(k\phi)\,, \quad k = 2,4,6,\ldots \quad (8)$$

for the "angular" wavefunctions with either positive or negative parity.

For the quantum numbers $n = 0,1,2,\ldots$ and $k = 1,2,3,\ldots$ one chooses the lowest possible values to describe the yrast spectra. This means one takes always $n = 0$ and $k = 1$ for even angular momenta (positive parity) and $k = 2$ for odd angular momenta (negative parity).

3 Diagonalization of the Unrestricted Hamiltonian

Usually the fastest method to solve the Schrödinger equation is the grid method (finite differences). However, the diagonalization method is more efficient if an appropriate basis is chosen. This is especially true if the Hamiltonian matrix elements can be obtained in an analytic form. We use this advantage in the present approach. Although the diagonalization is performed numerically, the problem remains analytic in the mentioned sense. This guarantees a quite fast solution and outperforms the method of finite differences in calculation time.

3.1 Choice of the Basis

The CQOM has a boundary condition which leads to a separation of the left ($\beta_2 < 0$) and right ($\beta_2 > 0$) quadrupole-octupole deformation plane. The CQOM model only uses the right half-plane with prolate shapes. The above mentioned complete set of orthonormal eigenfunctions $\Phi(\eta, \phi)$, eq. (5), of the CQOM model provide a natural choice because they automatically take into account this boundary condition. Therefore we choose them as basis functions for the solution in the case of the two-dimensional quadrupole-octupole model (2DQOM) *without* coherence, *i.e.* allowing $\omega_2 \neq \omega_3$.

3.2 Details of the Numeric Algorithm

As a first step a basis truncation is performed since the basis space is infinite-dimensional. The quantum numbers n and k, at which the basis is truncated, are determined by imposing a certain limit on the energy in the CQOM expression eq. (3) for a given set of model parameters.

The basis functions are completely determined if the CQOM parameters b, c and d_0 are given. The values of these parameters should be chosen in an appropriate way. A suitable choice of them can reduce the number of basis states necessary for a certain precision to a minimum, *i.e.* the basis can be optimized. Since the parameters B_2, B_3, C_2, C_3, d_2, d_3 and d_0 can vary independently in the 2DQOM, there are in principle two choices, namely a quadrupole and an octupole one for b and c. For the parameter b one has for example

$$b_{\text{quad}} = \frac{2B_2}{\hbar^2 d_2} \quad \text{or} \quad b_{\text{oct}} = \frac{2B_3}{\hbar^2 d_3}\,. \tag{9}$$

We have then chosen the arithmetic mean $b = (b_{\text{quad}} + b_{\text{oct}})/2$ which means that no degree of freedom is preferred and in case of coherence ($b_{\text{quad}} = b_{\text{oct}}$) the parameter is chosen as in the CQOM model. A similar choice was done for the parameter c. The parameter d_0 can simply be taken over from the CQOM solution.

Then the integrals of the Hamiltonian matrix are calculated. As a first step, the Hamiltonian (1) has to be transformed to the ellipsoidal coordinates, eq. (2), see equation (11) in [8] for the kinetic part. The matrix elements depend on the

parameters B_2, B_3, C_2, C_3, d_2, d_3 and d_0 of this Hamiltonian. The integration is over the right half-plane only. The matrix elements for a fixed angular momentum are given by

$$\langle n'\, k'|H|n\, k\rangle_I = \\ = \frac{d}{\sqrt{d_2 d_3}} \int_{-\pi/2}^{\pi/2} \int_0^{\infty} \psi^I_{n',k'}(\eta)\varphi_{k'}(\phi) H(\eta,\phi) \psi^I_{n,k}(\eta)\varphi_k(\phi)\eta d\eta d\phi\,, \quad (10)$$

where the parity of the angular functions $\varphi_k^{\pm}$ is fixed by the quantum number k (odd or even). Since the integration is performed in the coordinates η and ϕ, the Jacobian from the transformation (2), $J(\eta) = \frac{d}{\sqrt{d_2 d_3}}\eta$, appears in the matrix elements (10). Then the integrations over the "radial" coordinate η are always reduced to the following known analytic expression [13]

$$\int_0^{\infty} t^{\alpha-1} e^{-pt} L_m^{\lambda}(pt) L_n^{\beta}(pt) dt = \frac{p^{-\alpha}\Gamma(\alpha)\Gamma(n-\alpha+\beta+1)\Gamma(m+\lambda+1)}{m!n!\Gamma(1-\alpha+\beta)\Gamma(\lambda+1)} \\ \times {}_3F_2(-m,\alpha,\alpha-\beta;-n+\alpha-\beta,\lambda+1;1)\,, \quad (11)$$

which is fast evaluated. The ϕ-integrations only involve trigonometric functions and are easily performed.

In order to obtain a two-dimensional matrix instead of the four component tensor, eq. (10), the basis functions are relabelled into a list with only one index. For a fixed angular momentum I the resulting matrix is diagonalized and we obtain the eigenvalues and eigenvectors. The corresponding physical state from the yrast band is determined by the lowest eigenvalue whose eigenvector possesses the correct parity $(-1)^I$. In this way the model spectrum is constructed. In the CQOM the yrast states are characterized by the quantum numbers $(n,k) = (0,1)$ for even I and $(0,2)$ for odd I. In the 2DQOM n and k are no longer good quantum numbers. Then the model eigenfunctions are characterized by their decomposition coefficients in the basis states. It was found that for a given eigenfunction the main decomposition component still corresponds to the quantum numbers of the respective state in the CQOM model. Other higher lying basis states are also mixed into the final eigenstate to a certain amount.

4 Application to some Rare-Earth Nuclei

Once the diagonalizations have been performed for all angular momenta, one obtains an yrast spectrum and is able to define a function σ_{RMS} which gives the root mean square deviation from the experimental levels. Then the model parameters B_2, B_3, C_2, C_3, d_2, d_3 and d_0 can be adjusted so as to provide the best description of experimental data. For this minimization procedure a first guess must be known. For this reason we take the known CQOM parameters ω and b (for the choice of c see next paragraph) and calculate a set of parameters B_2, B_3, C_2, C_3, d_2 and d_3 which corresponds to the same solution. (d_0 can simply be taken over from the CQOM solution.)

Table 1. Theoretical alternating parity spectra with energy staggering obtained by CQOM [8] (first column), present 2DQOM (second column) and experimental levels for ^{150}Nd [9], ^{152}Sm [10], ^{154}Gd [11] and ^{156}Dy [12].

I^π	CQOM	2DQOM	Exp	I^π	CQOM	2DQOM	Exp
		^{150}Nd				^{152}Sm	
1^-	777.30	830.33	852.94	1^-	853.73	917.93	963.354
2^+	112.46	109.67	130.21	2^+	112.23	103.58	121.782
3^-	921.50	945.62	934.86	3^-	994.59	1037.02	1041.114
4^+	358.23	353.48	381.45	4^+	357.52	336.44	366.479
5^-	1167.13	1147.55	1129.0	5^-	1235.09	1246.37	1221.48
6^+	707.63	705.61	720.4	6^+	706.33	680.19	706.88
7^-	1495.94	1426.88	1432.6	7^-	1557.94	1537.95	1505.61
8^+	1131.57	1135.83	1129.7	8^+	1129.65	1112.53	1125.35
9^-	1889.64	1771.67	—	9^-	1945.59	1901.56	1879.11
10^+	1607.52	1617.80	1599	10^+	1604.99	1612.06	1609.23
11^-	2332.69	2169.37	—	11^-	2382.93	2326.22	2326.96
12^+	2119.74	2131.90	2119	12^+	2116.62	2160.82	2148.51
13^-	2812.95	2608.46	—	13^-	2857.99	2801.37	2833.25
14^+	2657.61	2664.64	2682.5	14^+	2653.93	2744.76	2736.01
		^{154}Gd				^{156}Dy	
1^-	1035.45	1109.72	1241.271	1^-	1142.05	1207.65	1293.20
2^+	114.21	103.23	123.070	2^+	128.52	119.78	137.77
3^-	1175.71	1230.75	1251.625	3^-	1285.26	1336.46	1368.36
4^+	365.10	335.44	370.995	4^+	404.34	382.37	404.19
5^-	1416.66	1442.82	1404.069	5^-	1529.41	1559.21	1526.28
6^+	724.23	678.97	717.655	6^+	787.67	757.08	770.44
7^-	1742.56	1737.17	1674.10	7^-	1856.55	1863.01	1809.97
8^+	1162.85	1112.68	1144.43	8^+	1243.34	1213.05	1215.61
9^-	2136.90	2103.26	2040.50	9^-	2248.63	2233.70	2186.58
10^+	1657.97	1616.31	1637.04	10^+	1746.71	1725.72	1725.02
11^-	2584.87	2530.18	2482.28	11^-	2690.23	2657.99	2636.55
12^+	2193.06	2172.64	2184.67	12^+	2281.93	2277.46	2285.88
13^-	3074.38	3007.66	2981.27	13^-	3169.27	3124.51	3103.60
14^+	2756.75	2767.92	2777.30	14^+	2838.97	2856.07	2887.82
15^-	3596.01	3526.59	3519.07	15^-	3676.68	3624.05	3596.40
16^+	3341.28	3391.55	3404.44	16^+	3411.39	3453.12	3498.88
17^-	4142.60	4079.24	4102.0	17^-	4205.78	4149.33	4157.80
18^+	3941.28	4035.45	4016.1	18^+	3994.98	4062.66	4025.80
19^-	4708.78	4659.21	4735.5	19^-	4751.66	4694.73	4771.20
20^+	4553.01	4693.55	4646.3	20^+	4586.87	4680.43	4635.60

This set of parameters is not uniquely fixed since there are many CQOM potentials which all lead to the same energies. This is especially true for the present treatment of yrast spectra only. The parameter c enters only in the wave-

functions and is irrelevant for the energies. Its value governs the overall size of the parameters B_2, B_3, C_2, C_3, d_2 and d_3 and can therefore be chosen to provide a scaling of the parameters to an order of magnitude which is physically reasonable. Secondly, there are many choices for the ellipsoidal minimum which differ in excentricity. This can be used to reach a certain ratio of quadrupole to octupole parameters. We chose the parameter c as 100 and fix the excentricity in such a way that the minimum becomes a circle which implies $B_2 = B_3$, $C_2 = C_3$ and $d_2 = d_3$.

All calculations were done with 20 basis states. The truncation of the basis was done as described in section 3.2. It was verified that at the minimum position the resulting energy levels only vary insignificantly if more states are added to the basis, *e.g.* if 30 states are taken into consideration each level differs from the given levels in Table 1 by less than about 1 keV.

Table 2. Parameters of the fits obtained for ^{150}Nd, ^{152}Sm, ^{154}Gd and ^{156}Dy. The parameters B_2, B_3 are given in units of $\hbar^2$/MeV, C_2 and C_3 are given in units of MeV, d_2 and d_3 are given in $\hbar^2 \cdot \text{MeV}^{-1}$ and d_0 is given in $\hbar^2$.

Nucleus	B_2	B_3	C_2	C_3	d_2	d_3	d_0
^{150}Nd	8.936	112.581	177.719	122.471	1205.101	1406.955	30.577
^{152}Sm	7.247	84.032	190.110	154.241	1052.186	1215.422	64.251
^{154}Gd	16.155	57.355	218.904	168.194	1210.526	1341.800	79.806
^{156}Dy	36.249	59.798	170.942	149.937	1311.362	1550.467	39.230

The model approach was applied to describe the yrast alternating parity spectra of the nuclei ^{150}Nd, ^{152}Sm, ^{154}Gd and ^{156}Dy. In Table 1 the model levels obtained in the present calculations are compared to the experimental levels and to the levels obtained in the coherent case. The resulting minimum parameters are given in Table 2. A graphical comparison of the energy levels together with root mean square values can be seen in Figure 1.

5 Discussion and outlook

The results in Table 1 and the comparison of energy levels in Figure 1 show that the 2DQOM leads to a better description of the yrast spectra of all four nuclei under consideration. This is in agreement with our expectation since the numerical solution is a generalization and contains the analytical solution as a special case. The restriction to equal frequencies ω_2 and ω_3 is equivalent to certain relations between the model parameters (mass-, stiffness- and inertia parameters) which must hold and which lead to the four CQOM parameters ω, b, d_0 and c. The 2DQOM does not have these limitations and therefore consists of the seven parameters B_2, B_3, C_2, C_3, d_2, d_3 and d_0 which are all allowed to vary freely. It is clear that a larger number of parameters should lead to a better description.

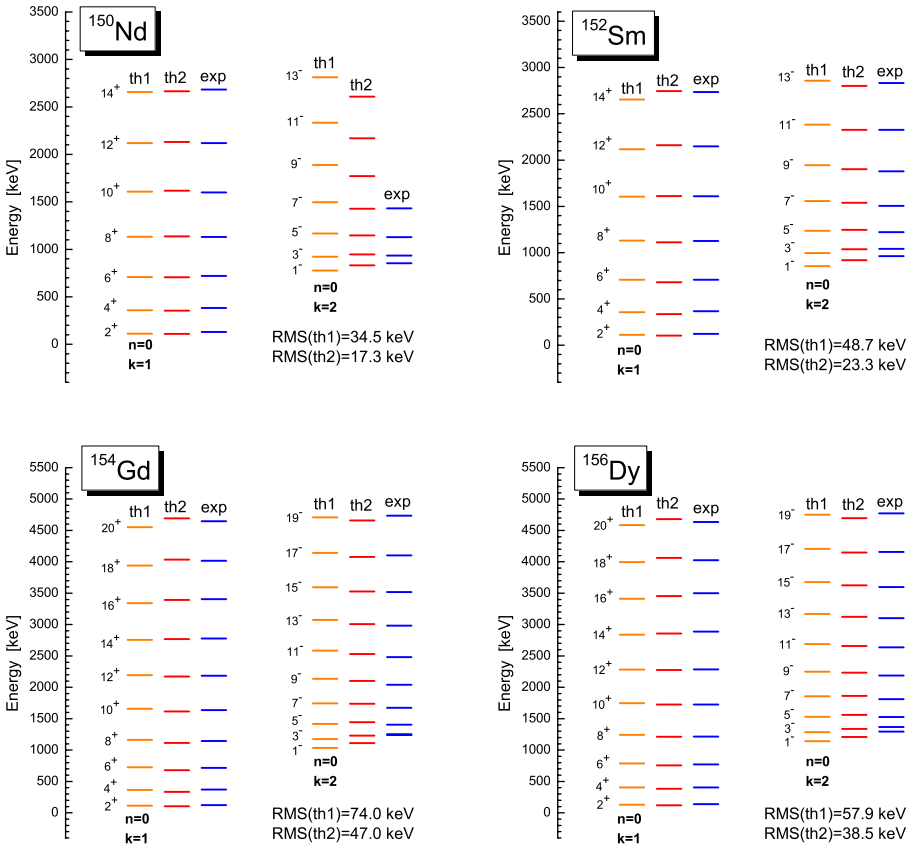

Figure 1. Theoretical levels obtained by CQOM [8] (th1), present 2DQOM (th2) and experimental levels for ^{150}Nd [9], ^{152}Sm [10], ^{154}Gd [11] and ^{156}Dy [12].

As mentioned in the last section, there are many choices of the parameters B_2, B_3, C_2, C_3, d_2, d_3 and d_0 which lead to the same energy levels. Therefore the model does not provide a unique potential shape. This freedom in the choice of the parameters could be used to satisfy additional conditions, *e.g.* one could demand a certain minimum position for the potential. In an extended ansatz which also treats transition probabilities the wave functions become important and the parameter c as well as the excentricity of the minimum can no longer be chosen arbitrarily.

Concerning future improvements, the inclusion of transition probabilities into the fitting procedure to describe them and the spectrum simultaneously is therefore of high interest. Secondly, one could look not only for yrast states but

also for higher lying states for which experimental data also exists. Thirdly, one could extend the formalism also to even-odd nuclei. Work in these directions is in progress.

Acknowledgements

This work is supported by DFG and HIC for FAIR. One of the authors (N. M.) acknowledges the support by the Bulgarian National Science Fund (contract DID-02/16-17.12.2009).

References

[1] A. Bohr, B.R. Mottelson, *Nuclear Structure*, vol. II, New York: Benjamin (1975).
[2] P.A. Butler, W. Nazarewicz, *Rev. Mod. Phys*. **68** (1996) 349.
[3] H.J. Krappe, U. Wille, *Nucl. Phys. A* **124** (1969) 641.
[4] R. Jolos, P. von Brentano, F. Dönau, *J. Phys. G: Nucl. Part. Phys.* **19** (1993) L151.
[5] R. Jolos, P. von Brentano, *Phys. Rev. C* **49** (1994) R2301.
[6] A.Ya. Dzyublik, V.Yu. Denisov, *Yad. Fiz.* **56** (1993) 30 [Phys. At. Nucl. **56**, 303 (1993)].
[7] V.Yu. Denisov, A.Ya. Dzyublik, *Nucl. Phys. A* **589** (1995) 17.
[8] N. Minkov, P. Yotov, S. Drenska, W. Scheid, D. Bonatsos, D. Lenis, D. Petrellis, *Phys. Rev. C* **73** (2006) 044315.
[9] E. der Mateosian, J.K. Tuli, *Nucl. Data Sheets* **75** (1995) 827.
[10] A. Artna-Cohen, *Nucl. Data Sheets* **79** (1996) 1.
[11] C.W. Reich, R.G. Helmer, *Nucl. Data Sheets* **85** (1998) 171.
[12] C.W. Reich, *Nucl. Data Sheets* **99** (2003) 753.
[13] http://functions.wolfram.com/Polynomials/LaguerreL3/21/02/01/.